Solid friction in gel electrophoresis

S. F. Burlatsky[a] and John M. Deutch
Department of Chemistry, Massachusetts Institute of Technology, Cambridge, Massachusetts 02139

(Received 26 January 1995; accepted 14 June 1995)

We study the influence of solid frictional forces acting on polymer chains moving in a random environment. We show that the total reduction in the chain tension resulting from the small friction between a polymer and fixed entanglement points is a steep nonlinear function of the number of entanglements (exponential for stretched chains). Therefore, solid friction can drastically change the dynamics and lead to trapping of long chains with a large number of entanglements. We present explicit results for the decrease of the chain tension in the presence of solid friction forces, for the limiting tension values, and for trapping thresholds for charged chains in an external field. The trapping threshold increases with the decrease of the field strength and/or application of pulsed field sequences as compared to static high fields. Our theoretical results on trapping thresholds are in good agreement with experimental data on DNA electrophoresis. Our model also predicts new nonlinear dependencies for the velocity of charged chains that are dragged through the gel by external forces. We present explicit dependencies of the velocity on charge, external force and polymer length for charged chains in external fields and for chains dragged by external forces that are applied only to chain ends. These dependencies are different in large and small force (field) limits, which correspond to stretched and harmonic chains. The strong mobility on length dependence which results from solid friction forces can serve to separate long linear charged polymers of different molecular weight.

I. INTRODUCTION

There is considerable interest in understanding[1] the mechanism of DNA electrophoresis because of its importance to molecular biology; for recent reviews see Refs. 1–4. The separation of the charged polymer chains of different length is directly related to the characteristic time required for external electric field E to drag the charged chain through the fixed obstacles that characterize the gel. In previous theoretical work[5–17] and computer simulations[18–25] the mechanism responsible for the movement has been attributed to friction between the chain and the solvent as it moves along a random path defined by its conformation among the fixed obstacles in the gel network.

The conventional theory[5–17] describes correctly the main features of gel electrophoresis in static external field E: In certain length intervals the mobility of chain decreases as the inverse of the chain length L for the chains below some critical length, which depends on E, temperature T, and on gel concentration. At large L, the mobility becomes length independent. (See Ref. 26 for the discussion of the decline of mobility on length dependence for low fields and high gel concentration, where the chains are strongly entangled.)

Pulsed electrophoresis in which the direction of the forcing electric field alternates at regular intervals between a forward direction and a substantial orthogonal component or opposite direction, improved separation by a factor of approximately 100 compared to constant field electrophoresis.[27,28] However, the conventional theory does not adequately describe electrophoresis of long chains.[1–4,29] The most troublesome discrepancy between predictions of conventional theory and experiment is the behavior of large entangled chains.[3]

Separation of long chains is believed to be connected with strongly entangled chain configurations: so called Λ configuration,[14] ''U'' and ''J'' configurations,[12,15,16] ''zigzag'' or ''staircase'' (see p. 32 and Fig. 5 in Ref. 3) configurations. The length dependence of mobility that enables the separation arises from entanglements. According to Ref. 29, ''under a given set of electrophoretic conditions, *molecules larger than a threshold size become irreversibly entrapped in the gel matrix and fail to migrate.*'' The pulsed field increases the probability of entangled configuration and at the same time it can mobilize trapped chain. The freezing threshold N^* for entrapment is inversely proportional to the voltage gradient E.[29–31] According to Ref. 31 ''In high electric fields, megabase DNA fragments are found to be trapped, i.e., to enter or migrate in gel only very slowly, if at all.'' However the empirical dependence presented in Ref. 31 for $N^* \sim \exp(\text{const}/E)$, predicts that the freezing threshold approaches a constant when E tends to infinity. Irreversible entanglement of charged molecules in gel matrix has also been reported.[32]

The results of direct observation of charged polymers during electrophoresis[33] and the discrepancy of experimental data with conventional theory motivates a search for an additional type of interaction of polymer chain with a gel.[34] We[34] introduced an additional physical mechanism that should be important for relaxation of entangled long chains—*the solid friction between the segments of polymer chain and gel*. We have shown that for entangled configurations of the polymer chain the local solid friction is proportional to the local tension force and it reduces the mobility of an entangled chain by the factor which exponentially depends on the number of entanglements. Since the dry friction

[a]On leave from Institute of Chemical Physics, Russian Academy of Science. Present address: Department of Chemistry, BG-10, University of Washington, Seattle, Washington 98195.

 0021-9606/95/103(18)/8216/12/$6.00

coefficient for the fiber–chain interaction in the presents of the solvent is small, solid friction does not change the dynamics of short chains and of large chains with small number of entanglements. However, it can drastically change the relaxation behavior and lead to trapping of long chains with large number of entanglements.

The existence of forces of the similar type was predicted in Ref. 35. A microscopic picture for local pinning of a long polymer chain by a gel fiber, which on the mesocopic scale should lead to solid like friction forces[36] was presented in Ref. 10. In recent friction force microscopy experiments[37] the oscillating in time force, acting on individual molecules, which in average results in solidlike friction for the atomic scale motion, was detected. On the other hand, the experiments on DNA Electrodiffusion in 2D array of posts[38] indicated that under particular experimental conditions a simple post array (without solid friction effects) will probably not give rise to strongly dispersive electrophoretic mobility of polymers. Thus, the direct experimental observations[33,37,38] and the theoretical estimates[10] support the conclusion that solid friction forces should be important in gel electrophoresis.

In the present paper we derive the general result for the mobility of the stretched (ropelike) chain in arbitrary configuration, consider some simple examples of different chain configurations, analyze the mobility of harmonic chains, and present the results for the solid friction induced freezing threshold. The paper is organized as follows: In Sec. II we present the microscopic equations for tension and velocity with phenomenological friction force for each turning point at polymer–fiber contact; in Sec. III we derive the coarse grained functions which eliminate small scale chain fluctuations; in Secs. IV and V we apply these equations to a stretched and harmonic chains and in Sec. VI—to chains which are in ''close to stretched'' state.

II. MICROSCOPIC EQUATIONS FOR TENSION AND VELOCITY

In the conventional picture of electrophoresis an extended polymer chain, assumed to be uniformly charged, is dragged free from entanglement about a fixed gel point by the action of external electric field. In the absence of solid friction this picture is similar to the rope being pulled over a frictionless peg through a viscous medium; the velocity with which the rope is withdrawn is determined by a balance of the tension imposed by the external field and the viscous drag. In the presence of solid friction this velocity is reduced by rubbing force exerted at the point of contact between the moving rope and the fixed peg.

When a segment interacts with a gel point, the chain tension, induced by the external field, leads to the local pinning of the chain in metastable local minima of the chain–fiber interaction potential, which are produced by the inhomogeneity of the chain shape.[10] The longer the chain and the larger the field, the deeper is the local minima. Estimates presented in Ref. 10 show that the depth of these local minima is significant compared to the thermal energy for the experimental conditions described in Refs. 27 and 28. Falling from these metastable minima to a lower minimum causes fibers to become vibrationally exited, and the vibrational energy is dissipated as heat. On a semiphenomenological level, local pinning of a static chain and energy dissipation for moving chain result in rubbing friction (see Ref. 36 for the detailed discussion of the similar microscopic model for solid friction forces acting on monomer particles).

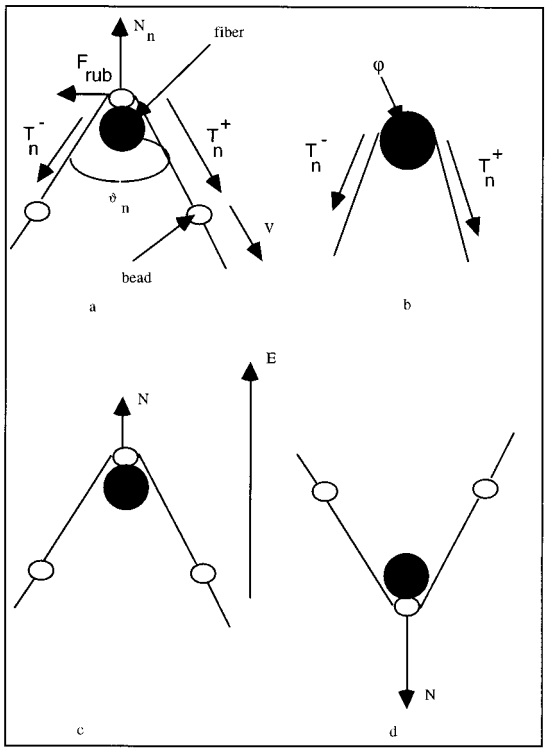

FIG. 1. Microscopic models: a—beads and springs model, b—Euler-type model; c and d present different orientations of the chain with respect to external field.

Some details of the phenomenological definition of the friction force depend on the microscopic model of the chain. For a bead and spring model of the chain [Fig. 1(a)], where a bead which is sliding along the gel fiber, is the source of solid friction, the microscopic magnitude of this friction force F_{rub} is

$$F_{\mathrm{rub}}(n)=\mu N_n,$$

$$N_n=\left[\pm qE_\perp+(T_n^-+T_n^+)\cos\frac{\vartheta_n}{2}\right],$$

$$\text{if } \pm qE_\perp+(T_n^-+T_n^+)\cos\frac{\vartheta_n}{2}\geqslant 0, \tag{1a}$$

$$N_n=0, \quad \text{if } \pm qE_\perp+(T_n^-+T_n^+)\cos\frac{\vartheta_n}{2}<0,$$

where n is the segment index, μ is the coefficient of sliding friction,[39] $E_\perp$ is the normal electric field, N_n is normal force, exerted by the gel point on the polymer segment. The latter force is equal to the projection of the sum of all forces acting on the segment to normal direction at the point of bead–fiber contact. The sign of the qE term is determined by the orientation of E with respect to N_n [see Figs. 1(c) and 1(d)], T_n^+

and T_n^- are the tension forces imposed by the left and right neighboring springs, and ϑ_n is the angle between these two springs, $0<\vartheta(r)<\pi$. For small friction coefficient, $\mu \ll 1$, $T_n^+ \approx T_n^- \approx T_n$.

For gel points with a diameter much bigger than b, the chain can be approximately treated as a rope wrapped around a macroscopic obstacle [see Fig. 1(b)]. For this model one has a famous Euler result for solid friction force (without external field)

$$F_{\rm rub}(n)=T^+(n)[1-\exp(-\mu|\varphi|)], \tag{1b}$$

where φ is total wrapping angle, $0<\varphi<\pi$. For small μ it leads to $T^+ \approx T^- \approx T$ and

$$F_{\rm rub}(n)=T(n)\mu|\varphi|. \tag{1c}$$

The above models are a simplification of the local interaction of the fiber and the chain; we have adopted a macroscopic friction description for microscopic interaction. However, only the following common main features of these models are important for dynamics of the chain: (1) The solid friction force is opposite to the velocity direction; (2) it increases proportionally to the tension forces and it varies with the angle which the chain makes in the interaction point. In a coarse grain description, which will be treated below, there is no significant difference between the two microscopic solid friction models exhibited.

In steady state the projection on the path of all forces acting on monomer is equal to zero. For a monomer *which interacts with a fiber* it leads to

$$\beta v + F_{\rm rub} + (T_{n+1} - T_n) - qE\ \cos(\Theta_n)=0, \tag{2}$$

where βv is friction force exerted by the solvent on the moving segment, β is friction coefficient of each segment, Θ_n is the angle between the external field and the direction of chain motion, and v and q are the velocity and charge of chain segment. Directions of all forces are presented in Figs. 1(a) and 2.

Not each segment will interact with a gel point, if the persistent polymer segment size "b" is smaller then the characteristic separation between gel points "a." Let us introduce interaction probability function

$$\epsilon(n,t)=\sum_i \delta(n-k_i), \tag{3}$$

where δ is the delta function for the continuous model and the Kronecker function for discrete chain, and k_i are successive numbers of segments which interact with gel fibers. For the discrete model $\epsilon(n,t)$ is equal to zero, if the segment with the number n does not interact with any gel fiber, and it is equal to unity if it does. For example, for the configuration of beads and springs presented on Fig. 3—$k_1=1$, $k_2=4$, $k_3=12$.

In the continuous limit, we obtain the following equation for the projection on the chain path of all forces acting on an *arbitrary* monomer

$$\beta v + \mu\epsilon(r)[T(r)\alpha(r) \pm qE\ \sin\ \theta(r)] + \frac{dT(r)}{dn} - Eq\ \cos\ \theta(r)=0, \tag{4}$$

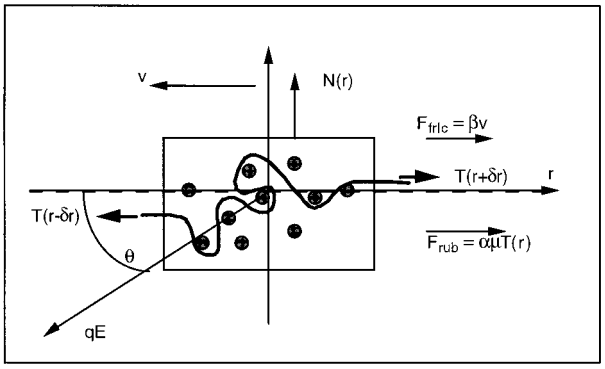

FIG. 2. The direction of various forces acting on a coarse grained element of the polymer chain. The steady-state segment velocity is in the $(-r)$ direction so the frictional force $F_{\rm rub}$ and $F_{\rm fric}$ are in $(+r)$ direction. The distance δr is along the coarse grained polymer chain.

For the bead and spring model—$\alpha(r)=2\cos(\vartheta(r)/2)$, for the Euler-type model—$\alpha(r)=|\varphi|$. If the chain does not change direction at given point, $\vartheta(r)=\pi$ and $\cos\vartheta=0$ for bead and spring model or $\varphi=0$ for Euler type model, and therefore $F_{\rm rub}=0$. The chain makes different angles $0<\vartheta(r)<\pi$ $(0<\varphi<\infty)$ at the interaction points. It is important that both $\cos[\vartheta(r)/2]$ and $|\varphi|$ are always non-negative contrary to $\cos\Theta$, which can have arbitrary sign. The function $\alpha(r)$ can not become negative, since tension forces only push the chain down to the obstacle in turning points of the primitive path, where chain–fiber interaction occurs [see Figs. 3 and Fig. 1(c) and 1(d)]. Let us also note that α is a measure of entanglement for one chain–fiber interaction and $\alpha\mu$ is a measure of solid friction resistance per interaction for given chain configuration.

Boundary conditions for Eq. (4) are determined by the external forces T_0 and T_N, acting on the chain ends

$$T(0)=T_0, \tag{4a}$$

$$T(N)=T_N. \tag{4b}$$

These conditions allow one to determine v for given end forces from Eq. (4).

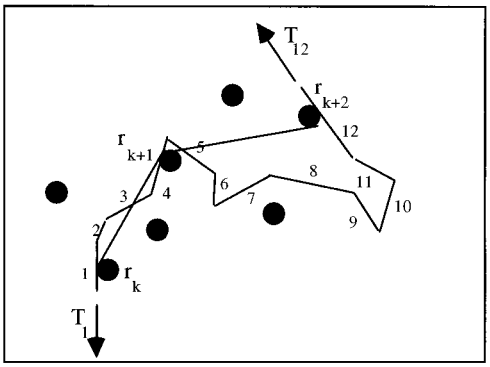

FIG. 3. A fragment of a chain. Solid line—chain segments, dashed line—primitive path.

In gel electrophoresis the chain can be found in coiled state, which exhibits harmonic properties and in extended stretched state.[10–12,14–24] We define, $\rho(r)\equiv dn/dr$, a linear density of the chain along the path coordinate r. By the definition it is equal to a number of segments per unit length along the primitive path. For stretched (ropelike) chain $\rho=$constant$=1/l$, where l is maximum segment size; for a elastic chain, ρ is a function of r.

The solution of Eq. (4) with boundary condition (4a) is a nonlinear functional of ϵ, ρ, α, Θ, and v. The solution[34] is

$$T(r)=\psi(r)T_0+\int_0^r \psi^{-1}(x)\{qE[\cos\ \theta(x) \pm \epsilon\mu\ \sin\ \theta(x)]-\beta v\}\rho\ dx, \tag{5}$$

where

$$\ln\ \psi(r)=-\mu\int_0^r \epsilon(x)\alpha(x)\rho(x)dx.$$

III. COARSE GRAINED FUNCTIONS

We introduce a mean-fieldlike approximation for coarse grained (with coarse graining distance $\delta r \geqslant a$) functions for the chain in the lattice of obstacles. The definition of the coarse grained function $f(r)$ is

$$f(r)=\frac{1}{\delta}\int_r^{r+\delta} f(x)dx, \tag{6}$$

where δ is the coarse graining distance longer than a, the average distance between gel points (see Fig. 2).

In order to calculate coarse grained ϵ, we choose $\delta r=a$ and consider a fragment of the chain, which is located between the fiber with path coordinate r and the next along the primitive path fiber with path coordinate $r+a$. The coarse grained interaction probability $\epsilon(r)$ is equal to the ratio of the number of the segments with path coordinates x, $r<x<r+a$, which interact with gel points, to the total number of the chain segments within this interval. Two of the segments of a given chain fragment are subject to solid friction force if the segment size is bigger then a fiber diameter[40] and smaller then a distance between gel points, see Fig. 3. Since both segments are at the boundary of the coarse graining interval, only one is included in the number of interactions for the interval, the other segment contributes to the neighboring interval. Therefore the number of interactions for this interval is one, and ϵ equals to inverse number of the chain segments for this fragment, which in turn is determined by the coarse grained linear density ρ. Since the number of chain segments between two successive obstacles is approximately equal to ρa, for coarse grained ϵ and ρ we obtain

$$\epsilon^{-1}=\rho a. \tag{7}$$

Formally one can write

$$\int_{k_i}^{k_{i+1}} \epsilon(n)dn=1, \tag{8}$$

since the function $\epsilon(n)$ is equal to zero for all n in the interval $k_i<n<k_{i+1}$, and

$$\int_{k_i}^{k_{i+1}} [\delta(n-k_i)+\delta(n-k_{i+1})]dn=1. \tag{9}$$

After the substitution, $dn=\rho\ dr$, we obtain

$$\int_{k_i}^{k_{i+1}} \epsilon(n)dn=\int_{r(k_i)}^{r(k_{i+1})} \rho(x)\epsilon(n(x))dx, \tag{10}$$

where $r(k)$ is the coordinate of kth obstacle along the chain path. Substituting local functions $\rho(x)$ and $\epsilon(x)$ by corresponding coarse grained values, $\rho(r)$ and $\epsilon(r)$, which are x independent on a length scale smaller then a, and taking advantage of the definition of the distance between two neighboring obstacles along the chain path: $r(k_{i+1})-r(k_i)=a$, we obtain Eq. (7) for coarse grained functions.[41] Note that for a completely stretched chain with $\rho=1/l$, interaction probability $\epsilon=l/a$, which equals to the number of segments of primitive path (interaction points), L/a, divided by the total number of chain segments, $N=L/l$, where L is entire chain length.

Since the function $\alpha(r)$ in Eqs. (1), (4), and (5) is nonnegative [in contrary to $\cos(\Theta)$], $\psi(r)$ in Eq. (5) is a monotonic function and one can introduce a mean function α for a coarse grained element of polymer chain. Strictly, the value of α will depend on the history of the chain in electric field.[34] After a long time in a large static field the long chain will approach complete elongation and α will approach zero. In a pulsed electrophoretic experiment, the chain has a random orientation at the beginning of the first pulse and α is approximately $2/\pi$ radian. The entangled configurations which are usually created in pulsed electrophoresis are characterized by relatively large value of α.

The coarse grained form of Eq. (4) is

$$\beta v+\frac{1}{s\rho}[T(r)\pm qE\ \sin\ \theta(r)]+\frac{dT(r)}{\rho dr} -Eq\ \cos\ \theta(r)=0. \tag{11}$$

Here we introduce a "screening" length s, $s=a/\alpha\mu$, which determines the length scale of solid friction resistance forces. Equations (4), (5), and (11) are the central results of our analysis. In next sections, we shall apply these results to stretched and harmonic chains.

IV. STRETCHED CHAIN

For a stretched (ropelike) chain $\rho=$const. and $n=\rho r$. The solution[34] of Eq. (11) with the boundary condition (4a) for a stretched chain and constant v is

$$T(r)=\exp\left(-\frac{r}{s}\right)\left\{T_0+qE\int_0^r \exp\left(\frac{x}{s}\right)\cos\ \theta(x)\rho\ dx +\beta v s\rho\left[\exp\left(\frac{L}{s}\right)-1\right]\right\}. \tag{12}$$

Here we ignore the term with the alternating sign, $\pm qE\ \sin\ \theta(r)$, because its sign change will average to zero along the chain when there are entanglements.

The velocity v is determined from the second boundary condition (4b), which leads to

$$\beta v \rho s = \frac{\exp(-L/s)T_0 - T_L}{1-\exp(-L/s)} + \frac{qE\int_0^L \exp(x/s)\cos\,\theta(x)\rho\, dx}{\exp(L/s)-1}. \quad (13)$$

Since L/a is equal to the number of segments of primitive path, i.e., to a total number of chain–fiber solid friction interactions, and $\alpha\mu$ is a measure of effective friction coefficient for one segment to fiber contact, $L/s=\alpha\mu L/a$, represents a measure of solid friction resistance for the stretched chain in a given configuration.

For $\alpha\mu=0$, v approaches the correct free draining limit

$$\beta v = [qEh + \rho^{-1}(T_0 - T_L)]/L, \quad (14)$$

where

$$h = \int_0^L \cos\,\Theta(x)dx \quad (15)$$

is the projection of the chain on the field direction.

For the chain with free ends, $T_0=T_L=0$, elongated in *straight* configuration $\cos(\Theta)=$const., and no tension is introduced along the chain. The flux determined by Eq. (13) for this case in the presence of solid friction, is equal to

$$\beta v = qE\,\cos(\Theta), \quad (16)$$

i.e., it is the same as the flux for the chain without solid friction.

Note that Eq. (13) is not symmetrical with respect to chain ends, since the direction of v determines the direction of friction force. The chain leaks from the end $r=L$ to the beginning $r=0$. Equations (12) and (13) are valid only if $v>0$.

If there is no external field (or chain charge), i.e., if E (or q)$=0$, the dependence of tension on path coordinate, $T(r)$, in Eq. (12) exponentially decreases from T_0 to T_L. Thus, the tension force T_0 (but not T_L) is screened by the effect of solid friction. *Random chains that are longer then the screening (or threshold) length $s=a/(\alpha\mu)$ experience an exponentially small tension and accordingly distant segments will not be moved by any externally applied force—the chain cannot be pulled out of the tube*. In such a case an exponentially small but finite force T_L will keep the chain in the tube.[42] In real systems such force could be provided by chain stiffness or/and by fluctuation-induced effects.

The steady state segment velocity for the chain leaving at $r=0$ with free end, $T_L=0$, and $E=0$ is equal to

$$\beta v = \frac{T_0}{\rho s[\exp(L/s)-1]}, \quad (17)$$

which approaches correct free draining limit $v=T_0/(\beta\rho L)$ if μ tends to zero. The first terms on the right-hand sides of Eqs. (12) and (13) provide a straightforward analog of the Euler result. In the Euler case absolute value of $\mu\varphi$ is a measure of solid friction resistance for the rope wrapped around a single obstacle, while, $L/s=\alpha\mu L/a$, is a measure of solid friction resistance for a chain that makes random angles.

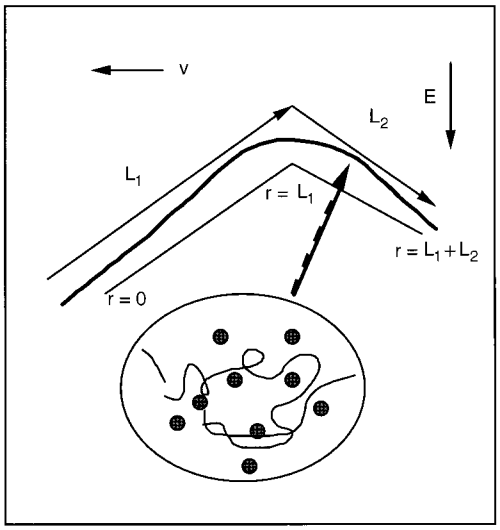

FIG. 4. Polymer chain in "Λ" configuration. The electric field E pulls the chain in the direction of lengthening L_2. The in set indicates that on smaller length scales the chain has achieved more favorable conformations with respect to the gel points and provides an averaged value of α.

A. "Λ" configuration: Dynamic case

We consider now in more detail the simplest particular conformation of the coarse grained chain with free ends—so-called "Λ" configuration[14] depicted in Fig. 4. In symmetrical "Λ" configuration with two arms of the chain, which make symmetrical constant angles with respect to the electric field, $\cos[\Theta(r)]=-\cos(\Theta)$ for $0<r<L_1$ (i.e., for the left, leading, arm of the chain) and $\cos[\Theta(r)]=\cos(\Theta)$ for $L_1<r<L_1+L_2$ (i.e., for the right, trailing, arm of the chain); and $\Theta=$constant. For this configuration Eq. (13) reduces to

$$\beta v = qE\,\cos\,\theta\left(\frac{2-\exp(-L_1/s)-\exp(L_2/s)}{\exp(L_2/s)-\exp(-L_1/s)}\right). \quad (18)$$

Note that this expression is not symmetric in L_1 and L_2. It corresponds to the physical case where $v>0$ in the direction indicated in Fig. 4. It follows that L_1 must be greater then L_2. In the limit $\mu\to 0$, the flux approaches

$$\beta v = qE\,\cos\,\Theta\,\frac{L_1-L_2}{L_1+L_2}, \quad (19)$$

which is the expected result.[15]

In the opposite limit if L_2 is large enough (but smaller than L_1) the chain will remain *frozen* in gel. *In contrast to a chain without charge, a charged chain in the given configuration can be trapped without any external forces acting on chain ends*. Consider the extreme case when L_1 tends to infinity. According to Eq. (18), the flux vanishes when the solid friction coefficient reaches the value:

$$L_2 = s\,\ln(2). \quad (20)$$

This result can be understood by noting that as the leading arm becomes infinitely long, its net effect is to place a

tension at the apex point, at the end of the trailing arm. In the presence of the solid friction this tension approaches a limiting value

$$T_{\lim}=\rho s(qE\ \cos\ \Theta-v\beta). \tag{21}$$

Equation (13) for the trailing arm with boundary conditions

$$T(L_1)=T_{\lim}, \tag{22a}$$

$$T(L_1+L_2)=0, \tag{22b}$$

leads to Eq. (20) as v tends to zero. Note that without solid friction $T_{\lim}$ increases as a linear function of L_2, i.e., *solid friction provides screening of tension and therefore introduces a finite limiting value for the tension of entangled chains.*

B. "Λ" configuration: Static case

Let us consider the chain in the nonsymmetrical[43] "Λ" configuration. In this configuration the leading and the trailing arms make different angles with the field. We examine the static case, when v equals zero. In this case the solid friction force acting on a segment is directed opposite to the direction of a *possible move* of this segment, i.e., is opposite to the projection on the chain path of all other forces. Let us introduce a turning point, with a coordinate along the primitive path $r=L_1+x$. At this point the solid friction force changes its direction. For the segments with path coordinate smaller than x, the direction of possible move is the same as indicated in Fig. 4. For the segments with path coordinate larger then x, the direction of possible move is opposite to the direction indicated in Fig. 4. Location of the turning point tends to the end of trailing arm, i.e., x tends to L_2, when the movement of the whole chain begins and static description becomes invalid. The equations for $T(r)$ read

$$\begin{aligned}
&\frac{T}{\rho s}+\frac{dT}{\rho\ dr}-Eq\ \cos\ \theta_1=0 \quad 0<r<L_1,\\
&\frac{T}{\rho s}+\frac{dT}{\rho\ dr}+Eq\ \cos\ \theta_2=0 \quad L_1<r<L_1+x,\\
&-\frac{T}{\rho s}+\frac{dT}{\rho\ dr}+Eq\ \cos\ \theta_2=0 \quad L_1+x<r<L_1+L_2.
\end{aligned} \tag{23}$$

Note the sign before the solid friction term $T/\rho s$. Equations (23) together with free ends boundary conditions,

$$T(0)=T(L_1+L_2)=0, \tag{24}$$

continuity equations for tension at the apex point,

$$\lim_{\epsilon\to 0}\ T(L_1-\epsilon)=\lim_{\epsilon\to 0}\ T(L_1+\epsilon), \tag{25}$$

and continuity equations for tension at the turning point,

$$\lim_{\epsilon\to 0}\ T(L_1+x-\epsilon)=\lim_{\epsilon\to 0}\ T(L_1+x+\epsilon), \tag{26}$$

lead to exponential change in $T(r)$: growth from $T(r)=0$ at beginning point to

$$T(L_1)=s\rho E\ \cos\ \theta_1 q[1-\exp(-L_1/s)] \tag{27}$$

at apex point, decrease to

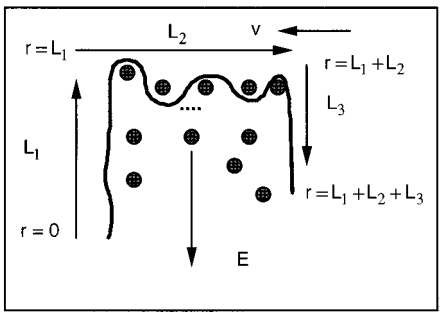

FIG. 5. Polymer chain in U-shaped configuration with unequal arms caught over gel points. The external field is directed downward.

$$T(L_1+x)=s\rho E\ \cos\ \theta_2 q\{1-\exp[-(L_2-x)/s]\} \tag{28}$$

at turning point, and then decrease to zero at the end point. The turning point location is

$$x=L_2+s\ \ln\left(1-\sqrt{1-\exp\left(-\frac{L_2}{s}\right)\left\{1+\frac{\cos\ \theta_1}{\cos\ \theta_2}\left[1-\exp\left(-\frac{L_1}{s}\right)\right]\right\}}\right). \tag{29}$$

For a symmetrical case with $\Theta_1=\Theta_2$ and $L_1=L_2$, the turning point coincides with the apex point: $x=0$, which means that the possible move direction for the left arm is to the left, and for the right arm is to the right. The static solution exists if the argument of square root in right side of Eq. (29) is nonnegative. For symmetrical configuration, with $\Theta_1=\Theta_2$, and with large leading arm, $L_1\gg s$, the static solution exists only if

$$L_2>s\ \ln(2), \tag{30}$$

i.e., under mobility threshold, which is predicted by Eq. (20). For large L_1 and L_2, L_1, $L_1\gg a/(\alpha\mu)$, the turning point location is of the order of screening length:

$$x=s\ \ln\frac{\cos\ \theta_2+\cos\ \theta_1}{2\ \cos\ \theta_2}. \tag{31}$$

If x becomes larger then L_2, the chain starts to move. *When $\cos\Theta_2$ tends to $\pi/2$, x tends to infinity, which means that change in the field orientation can "unfreeze" the trapped chain.*

C. "U"-shaped configuration

The influence of solid friction on the dynamics of stretched chains in other situations can also be investigated. For example, a long polymer chain, where the arms are leaking from the end of entangled region, as depicted in Fig. 5, corresponds to "U"-shaped configuration,[12,16] which presents a physical situation envisioned in most of lattice computer simulation studies.[10,15,18–22] Similar configurations have been observed experimentally.[33,44] In this situation the effect of solid friction is only present on the central arm

which is oriented perpendicular to the electric field and therefore $T(r)$ for the stretched chain can be determined from Eq. (5) with

$$\ln \psi(r)=0, \quad \text{for } 0<r<L_1 \quad \text{and}$$

$$\text{for } L_1+L_2<r<L_1+L_2+L_3, \tag{32a}$$

$$\ln \psi(r)=(r-L_1)/s \quad \text{for } L_1<r<L_1+L_2. \tag{32b}$$

Substituting these functions and using the free ends boundary conditions,

$$T(0)=T(L_1+L_2+L_3)=0, \tag{33}$$

we obtain

$$\beta v=qE\left[\frac{L_1\ \exp(-L_2/s)-L_3}{L_1\ \exp(-L_2/s)+L_3+s[1-\exp(-L_2/s)]}\right]. \tag{34}$$

If $L_1>L_3\ \exp[L_2/s]$ the chain will move with a velocity that extends the larger arm L_1 until the chain leaks from the entangled region. However, if $L_3<L_1\ll L_3\ \exp[L_2/s]$ then the solution to Eq. (11) is $v=0$ indicating that *the chain is frozen*.[42] There is no value of external electric field that can overcome the solid friction from the entangled region for given configuration.

Again we conclude that *solid friction predicts freezing of entangled configuration of long chains; this freezing does not arise in the conventional picture*. In the limit of perfectly stretched chains which was considered in present section the threshold of freezing, which is presented by Eq. (20) and Eq. (30) and can be extracted from Eq. (34), does not depend explicitly on E.

In the limit of no friction, $\mu=0$, Eq. (34) leads to the expected result:[15,16,18]

$$\beta v=qE\ \frac{L_1-L_3}{L_1+L_2+L_3}, \tag{35}$$

which shows that the flux is proportional to the difference in length of the dangling chain ends along the field direction. If L_2 tends to zero, the expression for v in Eq. (34) reduces to the form of Eq. (35), without solid friction and $L_2=0$, as expected from simulation results of the chain trapped about a single gel point.[15,16,18] This reflects the fact that slowing down of chain leakage from solid friction only occurs when there is entanglement over large distance.[45] Previous work has assumed that slow mobility arises from a small net electric force due to close initial length of the arms of the chain wrapped about a single gel obstacle. However, simple estimates[38] also show that these configurations are unstable, and, therefore, can not significantly change the mobility. The direct observations[33] show that such configurations soon slip off. In contrast, open circular DNA migrates much more slowly[46] which we attribute to entanglement and resulting solid friction.

The experimental significance of solid friction is clearly illustrated by the result of leakage from ''U'' configurations. Successful separation requires length dependence of the mobility μ_{mob} and solid friction discriminates chains of different

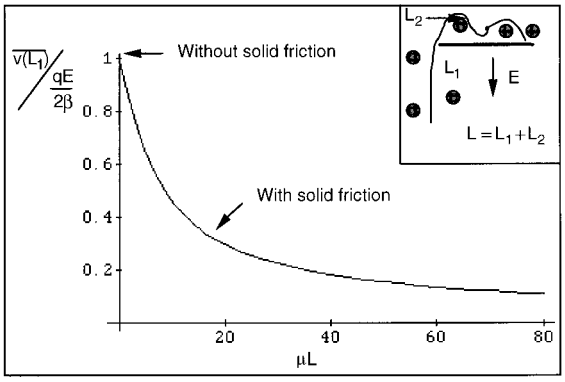

FIG. 6. Average flux for leakage from U-shaped polymer configuration in the gel. The leakage begins with the entire polymer of length L aligned perpendicular to the field and ends with the entire polymer aligned parallel to the field.

length. The mobility is v/E where v is the average velocity over the length L_1 as the chain leaks from the entangled region. This average velocity is

$$\bar{v}=\frac{1}{L-L_{\text{lim}}}\int_{L_{\text{lim}}}^{L} dL_1 v(L_1), \tag{36}$$

where L_{lim} is the minimum length where leakage along L_1 begins and L is the total polymer chain length.

Consider the limiting case where $L_3=0$ and $L_{\text{lim}}=0$. *If there is no solid friction* then $\mu_{\text{mob}}=[q/2\beta]$ according to Eq. (36) which is of the same order as the free draining solution value and *independent of chain length*. On the other hand, *if solid friction is present*, then according to Eq. (35) there is significant reduction and length dependence of this averaged velocity and mobility as illustrated in Fig. 6.

Available experimental information[26] at low static fields but high gel concentration where strong entanglement is expected, indicates a decline of mobility with long chain length greater than predicted by biased reptation theory.[6–9,13]

Similar ''U''-shaped configurations should be important for the penetration of a chain into a gel. In this case the horizontal arm lies on the top of the gel and two vertical arms enter it at random penetration points. Contrary to the above case the horizontal arm is not entangled and the effect of solid friction is present only on the vertical arms. An external constant field forces the elongation of the larger vertical arm. The analysis of the influence of solid friction leads to the conclusion that the chain becomes trapped if the smaller horizontal arm is larger then the mobility threshold. Change in the direction of the field can ''unfreeze'' the chain.

V. HARMONIC CHAIN

A. Mobility of the chain driven by one end

In order to explain by example the main features of solid friction for an elastic chain let us consider Euler-type model presented in Fig. 7 for a small harmonic string, which is pulled around the obstacle by two frictionless ropes in the

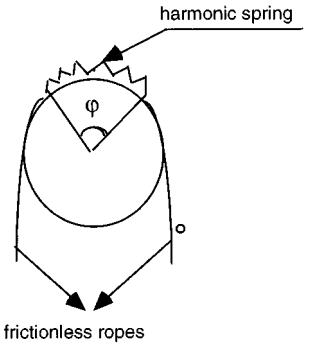

FIG. 7. A harmonic spring which is subject of solid friction is pulled around the obstacle by the frictionless ropes.

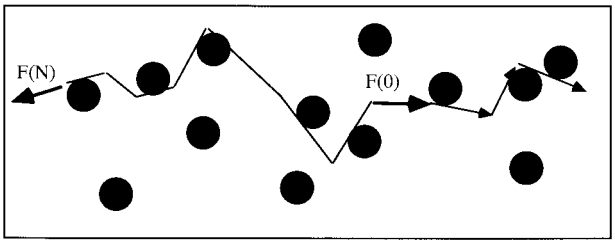

FIG. 8. Elastic chain driven through the gel by the external force $F(0)$. The set of arrows on the right from the leading chain end indicates that due to fluctuations and/or change of the direction of the force $F(0)$ the chain reproduces self similar entanglements.

small friction limit. For the harmonic string the Eq. (1c) remains valid. However, the angle φ gains a dependence on the tangential tension force

$$T=\gamma(\varphi-\varphi_0), \tag{37}$$

where φ_0 is the initial angle for zero tension, and $\gamma \propto \varphi_0^{-1}$ is the effective elasticity constant. By the substitution of the angle φ from Eq. (37) to Eq. (1c) we obtain

$$F_{\text{rub}}=\mu T\left[\frac{T}{\gamma}+\varphi_0\right]. \tag{38}$$

For the harmonic spring the increase of tension leads to the elongation of the spring, and therefore, to the increase of the angle φ, and simultaneously leads to the increase of normal reaction force. Therefore, the dependence of a frictional force on tension (38) is nonlinear.

For successive harmonic springs with coordinates r_i the tension is a linear function of the distance between the neighboring segments

$$T=\gamma\,(r_{i+1}-r_i-\lambda_0), \tag{39}$$

where l_0 is the equilibrium length of a spring and the effective elasticity γ is inverse proportional to l_0. In the continuous limit

$$\rho^{-1}=\frac{dr}{dn}=r_{i+1}-r_i, \tag{40}$$

which leads to the following dependence of linear density on tension

$$\rho=\frac{1}{T/\gamma+l_0}. \tag{41}$$

Substitution of this expression for the density in Eq. (11) leads to

$$\beta v+\frac{T(T/\gamma+l_0)}{s}+\frac{dT}{dn}-qE\,\cos\,\theta=0. \tag{42}$$

For a harmonic polymer chain, the elasticity arises from entropy effects. In this case, $l_0=0$, the effective elasticity constant $\gamma=3W/b^2$, where W is thermal energy and $W=$Boltzmann's constant times the temperature.[47] Thus, for the harmonic chain, we found

$$\beta v+\frac{T^2}{\gamma s}+\frac{dT}{dn}-qE\,\cos\,\theta=0. \tag{43}$$

For the harmonic chain, the increase of tension leads to the elongation of the chain, and therefore, to the increase of the number of contacts with fibers, and simultaneously leads to the increase of the normal reaction force for each contact. Therefore the solid friction term on the right-hand side of Eq. (43) is proportional to the square of the tension force.

First consider a chain with q (or E)$=0$, which contains N segments. The chain is pulled at the right leading end by the constant force $F(0)$ through an entangled region, as depicted in Fig. 8. We suppose that during the motion the chain reproduces similar entanglements. The solution of the Eq. (43) with $qE=0$ is

$$\frac{\arctan[T(n)/\sqrt{\gamma s\beta v}]}{\sqrt{\beta v/\gamma s}}=A-n, \tag{44}$$

where A and v are determined by the boundary conditions Eqs. (4a) and (4b) with $T_0>T_N$. We examine the different regimes of motion.

1. Small tension

For small tension, when

$$T_N<T_0 \tag{45}$$

and

$$T_0\ll\sqrt{\gamma s\beta v}, \tag{46}$$

we expand arctan in Eq. (44) for small argument and obtain the correct free dragging limit

$$\beta v=[T_0-T_N]/N. \tag{47}$$

Substitution of Eq. (47) into Eq. (46), leads to the criteria of small tension

$$T\ll T^*, \tag{48}$$

where T^* is the *critical tension,*

$$T^*=\gamma s/N, \tag{49}$$

which equals the tension, which stretches the elastic chain, that contains N harmonic springs, to the screening length s.

2. High tension, $T_0 > T^*$, at the leading end of the chain and zero tension $T_N = 0$, at the trailing end of the chain

The asymptotic expansion for arctan for large argument leads to

$$v = \frac{\pi^2 \gamma s}{4\beta (N + \gamma s/T_0)^2}. \tag{50}$$

The limiting velocity for $NT_0 \gg \gamma s$ is

$$\beta v = \frac{\pi^2 \gamma s}{4N^2} = \frac{\pi^2 W s}{4b^2 N^2}. \tag{51}$$

This limiting velocity is independent of T_0, decreases as N^{-2}, and depends on both friction coefficients β and $\alpha\mu$. It is approximately equal to the chain velocity which should be produced by the critical tension Eq. (48) in the free dragging limit (47). The result predicted by the Eq. (51) is unusual because the limiting velocity is independent of the force. We present below a qualitative analysis of Eq. (43) for a more general case.

3. High tension at the leading end of the chain, $T_0 \gg T^*$, and low tension at the trailing end, $T_N \ll T^*$.

We denote the number of segments in the vicinity of the leading chain end as n_1. For these segments the tension is high. We denote the number of the segments in the vicinity of the trailing chain end as n_2. For these segments the tension is low. In order to obtain a qualitative estimate for the velocity we assume that there is a sharp boundary between the high tension region and the low tension region and, therefore, that $n_1 + n_2 = N$.

For the leading end of the chain, $0 < n < n_1$, the tension is high, and therefore the solid friction term, $T^2/\gamma s$, is larger than the solvent friction term, βv, and Eq. (43) (with $qE = 0$) can be approximated as

$$\frac{T^2}{\gamma s} + \frac{dT}{dn} = 0. \tag{52}$$

The solution of Eq. (52) decreases as

$$T(n) = \frac{T_0}{nT_0/\gamma s + 1}. \tag{53}$$

For

$$n \gg \gamma s/T_0 \tag{54}$$

$T(n)$ loses its dependence on T_0, and the net tension, which the end of the high tension fragment of chain places at the beginning of the low tension fragment of the chain is equal to

$$T(n_1) = \gamma s/n_1. \tag{55}$$

For the low tension region, Eq. (43) reduces to

$$\beta v + \frac{dT}{dn} = 0 \tag{56}$$

with boundary conditions $T(N) = T_N$ and $T(N - n_2) = T(n_1)$. The solution is

$$\beta v = \frac{T(n_1) - T_N}{n_2}. \tag{57}$$

At the boundary between high and low tension regions, the solvent friction term βv is equal to the solid friction term, $T^2/\gamma s$:

$$\beta v = T(n_1)^2/\gamma s. \tag{58}$$

Taking advantage of Eqs. (55), (57), and (58), we obtain

$$n_1 = \frac{\gamma s}{T_N}\left(1 - \sqrt{1 - \frac{NT_N}{\gamma s}}\right). \tag{59}$$

For small T_N, this leads to

$$n_1 \approx n_2 \propto N/2 \tag{60}$$

and

$$\beta v \propto \frac{\gamma s - NT_N}{N^2}, \tag{61}$$

which coincides with Eq. (51) for $T_N = 0$.

Extrapolation of the results Eqs. (60) and (61) to intermediate trailing end tensions, $T_N \to \gamma s/N = T^*$, leads to $n_1 \to N$ and $v \to 0$. Thus for $T_N \to T^*$ the chain becomes frozen for arbitrary large tension, $T_0 > T_N$ at the leading end of the chain. For large leading end tension, $T_0 \gg T^*$, and small trailing end tension, $T_N \ll T^*$, the chain velocity is determined by Eq. (61) or Eq. (51) and does not depend on T_0 and T_N. For this case, the net effect of the increase of the external force is to increase the lengths of the chain segments in the small chain region containing n segments, $n < NT^*/T_0$ (n is much smaller then N since $T^* \ll T_0$), near the leading chain end. The dependence of v on T_0 vanishes, because the friction term for the given chain fragment increases with the increase of T_0, due to the elongation of the chain, which leads to an increase of the total number of interactions with the gel points. The increase of force is compensated by the consequent increase of solid friction. The velocity is inverse proportional to N^2, since the effective tension force (55), which drives the chain, and the net solvent–chain friction (57) are both inverse proportional to N [see Eq. (61)].

One can argue[48] that the harmonic chain approximation is inapplicable to long chains since the computer simulation indicates that long chains are aligned by the field and stretched. We estimate the validity of the pure harmonic approximation by considering an anharmonic chain with springs whose extension reaches a maximum value l when the tension tends to infinity. The harmonic approximation becomes invalid if T_0 is of the order of γl which is much smaller than the critical tension, T^*, if $N \gg \pi^2 s/l$. Therefore a sufficiently long chain can remain harmonic and at the same time exert high solid friction and obey the unusual dependence Eqs. (51) and (61). Note, however, that for long chains which perform reptation in tubes, the effective end tensile forces can provide high solid friction effects and complicate the chain dynamics. For the stretched chain, Eq. (21) shows that there is a limiting tension within the long entangled chain that will not be exceeded when the chain length increases. We now demonstrate a similar result for the harmonic chain.

B. "Λ" configuration

We consider a charged harmonic chain with $qE>0$ and with free ends in nonsymmetrical "Λ" configuration, see Fig. 4. Taking advantage of Eq. (43) we obtain the following equations of motion

$$\beta v+\frac{T^2}{\gamma s}+\frac{dT}{dn}-qE\ \cos\ \theta_1=0, \tag{62a}$$

$$\beta v+\frac{T^2}{\gamma s}+\frac{dT}{dn}+qE\ \cos\ \theta_2=0, \tag{62b}$$

for the left, leading, arm, $0<n<N_1$, and for the right, trailing, arm, $N_1<n<N_1+N_2$, correspondingly. For the leading arm the solution with zero boundary conditions at $n=0$ is

$$T(n)=f\,\frac{1-\exp(-\eta n)}{1+\exp(-\eta n)}, \tag{63}$$

where

$$\eta=2\sqrt{\frac{(qE\ \cos\ \Theta_1-\beta v)}{\gamma s}} \tag{64}$$

and

$$f=\sqrt{\gamma s(qE\ \cos\ \Theta_1-\beta v)}. \tag{65}$$

Note that for $\alpha\mu=0$ (or for small n) the frictionless limit

$$T=(qE\ \cos\ \Theta_1-\beta v)n \tag{66}$$

is regained. In the presence of solid friction, the tension of the harmonic chain approaches finite limit, which is equal to f, as n tends to infinity. *Thus, solid friction reduces the limiting tension in both cases, i.e., or stretched and harmonic chains.*[49]

The solution of Eq. (62b) (for the trailing arm) leads to

$$\frac{\arctan[T(N_1)/\sqrt{\gamma s(\beta v+qE\ \cos\ \Theta_2)}]-\arctan[T(n)/\sqrt{\gamma s(\beta v+qE\ \cos\ \Theta_2)}]}{\sqrt{(\beta v+qE\ \cos\ \Theta_2)/\gamma s}}=n-N_1. \tag{67}$$

Taking advantage of the zero boundary conditions, $T(N_1+N_2)=0$, and of large N_1 limit, which provides $T(N_1)=f$, we obtain for the velocity

$$\arctan\sqrt{\frac{qE\ \cos\ \Theta_1-\beta v}{\beta v+qE\ \cos\ \Theta_2}}=N_2\sqrt{\frac{(\beta v+qE\ \cos\ \Theta_2)}{\gamma s}}. \tag{68}$$

This equation does not have a positive solution if the number of segments in the trailing arm is greater then the threshold value, N^*,

$$N^*=\sqrt{\frac{\gamma s}{qE\ \cos\ \Theta_2}}\ \arctan\ \sqrt{\frac{\cos\ \Theta_1}{\cos\ \Theta_2}}$$

$$\approx\frac{\pi}{4}\ \sqrt{\frac{\gamma s}{qE\ \cos\ \Theta_2}}=\frac{\pi}{4}\ \sqrt{\frac{Ws}{b^2qE\ \cos\ \Theta_2}}. \tag{69}$$

Here an increase in the field leads to the decrease of the critical value of N_2. Note that N^* *tends to infinity when* $\cos\Theta$ *2 tends to* $\pi/2$ *which means that the change in the field orientation can "unfreeze" the trapped harmonic chain [compare with Eq. (31) for the stretched chain]. This suggests an explanation of the increase of penetration of long chains into gels in pulsed electrophoresis as compared to static field.*

Taking advantage of a commonly accepted estimate[6,8,11] for the typical cosine of the angle between the tube segment and external field in the limit of low, $qEa<W$, field:

$$\cos\ \Theta\approx qEa/kT, \tag{70}$$

we obtain

$$N^*\approx\pi W/4qEb\sqrt{\alpha\mu} \tag{71}$$

for the mobility threshold of harmonic chain.

The dependence on the temperature predicted by (70) is not apparent, since μ and α should depend on W. Also thermal fluctuations can significantly reduce trapping. Moreover, α will depend on E in different electrophoretic experiments. However *for a given conformation of the chain Eq. (70) explicitly predicts for* N^* *the same dependence on E as that has been experimentally determined.*[29] *An increase of gel concentration, external field or number of chain segments lead to the stretching of the chain. We assume, that the threshold on E dependence which was reported in Ref. 31 is the crossover to the field independent* value that is predicted by Eqs. (20) and (30) for perfectly stretched chain.

VI. TRAPPING THRESHOLD BEHAVIOR NEAR THE STRETCHED CHAIN LIMIT

For a perfectly stretched chain, Eqs. (20) and (30) predict a field independent trapping limit. This prediction agrees with experimental results. However the experimental dependence $N^*\sim\exp$ (const $/E$) (Ref. 31) contains much more information. Particularly, it predicts the high field limit

$$N^*\sim 1+\text{const}\ /E. \tag{72}$$

The chain in gel can be stretched by different physical reasons: small diameter of gel pores, tube fluctuations, segment rigidity and a high electrical field. We will examine only the high field in order to obtain a simple estimate for trapping threshold behavior.

The typical cosine of the angle between the external field and the chain, which is stretched by the field is equal to[6,8,11]

$$\langle\cos\ \Theta\rangle=\coth\left(\frac{qEa}{2W}\right)-\frac{2W}{qEa}. \tag{73}$$

For high fields, this leads to the typical value of the cosine which is of the order of unity. Note that for small fields it leads to Eq. (70) which we have used for harmonic chains.

For the Rouse bead and spring model with anharmonic springs the distance between two consecutive beads Δr is equal to

$$\Delta r = l\left(\coth \frac{bT}{W} - \frac{W}{bT} \right), \tag{74}$$

where b is Kuhn (segment) length of polymer; l is maximum spring length.[50] For small tensions it leads to harmonic behavior; for high tension it leads to

$$\Delta r \approx l\left(1 - \frac{W}{bT} \right). \tag{75}$$

In order to evaluate the trapping threshold behavior we shall examine a symmetrical Λ configuration, see Fig. 5, with an infinitely long leading arm in a static case. The trapping threshold can be determined as the maximum number of segments of the trailing arm, which can be confined by the net tension placed by the leading arm at the apex point. In this case the location of the turning point is at the end of the trailing arm. This leads to the zero boundary condition for the tension at this point.[51] In the continuous limit $\rho \approx (\Delta r)^{-1}$ [see Eq. (40)], Eqs. (11) and (75) lead to the following equations for trailing and leading arm:

$$\frac{l}{s}\left(T - \frac{W}{b} \right) + \frac{dT}{dn} - qE\cos\Theta = 0, \tag{76a}$$

$$\frac{l}{s}\left(T - \frac{W}{b} \right) + \frac{dT}{dn} + qE\cos\Theta = 0. \tag{76b}$$

As the leading arm tends to infinity, its net effect is to place the tension $T_{\lim}$ at the apex point. This limiting tension is determined by

$$\frac{l}{s}\left(T_{\lim} - \frac{W}{b} \right) = qE\cos\Theta. \tag{77}$$

By integration of Eq. (76b) for the trailing arm with boundary conditions

$$T(0) = T_{\lim}, \tag{78a}$$

$$T(N^*) = 0, \tag{78b}$$

we obtain

$$\ln \frac{qEb\cos\Theta - W\alpha\mu l}{2qEb\cos\Theta} = -\frac{l}{s}N^*. \tag{79}$$

In the high tension limit, which is under consideration here, we retain only the two first terms in the expansion of the left-hand side of Eq. (79). This leads to the result:

$$N^* = \frac{s}{l}\ln(2) + \frac{W}{qEb} + \cdots . \tag{80}$$

The first term in (80) is the same as the threshold limit for a completely stretched chain which is presented by Eqs. (20) and (30). The second term presents the relaxation to the limiting value, which agrees with experimental dependence (72).

VII. CONCLUSION

Thus, the theoretical results on trapping thresholds presented in this work, Eqs. (20), (71), and (80), are in good quantitative agreement with experimental data. Qualitatively our results agree with experimental results on gel dependence of electrophoretic mobility.[52,53] Our model predicts the following.

(1) The decrease of tension in presence of solid friction forces and presents explicit expressions for the limiting tension values Eqs. (63), (64), (77), and (21).
(2) The increase of the trapping thresholds with the decrease of the electric field and/or application of pulsed electrophoresis as compared to static high fields, Eqs. (20), (71), (80) and Eqs. (31), (69).
(3) New nonlinear dependencies for the velocity of charged chains, that are dragged through the gel by external forces, applied to chain ends and/or by an external field, acting on chain segments, for harmonic chains Eqs. (44), (51), (61) and for stretched chains Eqs. (13) and (17).

ACKNOWLEDGMENTS

One of us (J.M.D.) thanks George Whitesides for helpful discussions, S.F.B. thanks A. Yu. Grosberg, S. P. Burlatskaia, S. Granic, M. Moreau, G. Oshanin, J. L. Viovy, J. Shore, and J. Lebiwitz.

[1] See J. Maddox, Nature **345**, 381 (1990) and A. Khurana, Phys. Today **240**, 20 (August 1990) for popular accounts of theoretical developments.
[2] B. Norden, C. Elvingson, M. Jonsson, and B. Akermam, Q. Rev. Biophys. **24**, 103 (1991).
[3] J. L. Viovy, T. Dyke, and F. Caron, Contemp. Phys. **33**, 25 (1992).
[4] B. H. Zimm and S. D. Levene, Q. Rev. Biophys. **25**, 171 (1992).
[5] L. S. Lerman and H. L. Frisch, Biopolymers **21**, 995 (1982).
[6] O. J. Lumpkin and B. H. Zimm, Biopolymers **21**, 2315 (1982).
[7] O. J. Lumpkin, P. Dejardin, and B. H. Zimm, Biopolymers **24**, 1573 (1985).
[8] G. W. Slater and J. Noolandi, Phys. Rev. Lett. **55**, 1579 (1985); Biopolymers **25**, 431 (1986).
[9] J. Noolandi, J. Rousseau, and G. W. Slater, Phys. Rev. Lett. **58**, 2428 (1987).
[10] J. M. Deutsch, Phys. Rev. Lett. **59**, 1255 (1987); Science **240**, 922 (1988).
[11] J. L. Viovy, Phys. Rev. Lett. **60**, 855 (1988).
[12] J. Noolandi, G. W. Slater, H. A. Lim, and J. L. Viovy, Science **243**, 1456 (1989).
[13] P. Dejardin, Phys. Rev. A **40**, 4752 (1989).
[14] B. H. Zimm, Phys. Rev. Lett. **61**, 2965 (1988); J. Chem. Phys. **94**, 2187 (1991).
[15] J. M. Deutsch, J. Chem. Phys. **90**, 7436 (1989).
[16] H. A. Lim, G. W. Slater, and J. Noolandi, J. Chem. Phys. **92**, 709 (1990).
[17] J. M. Schurr and S. B. Smith, Biopolymers **29**, 1161 (1990).
[18] M. O. de la Cruz, J. M. Deutsch, and S. F. Edwards, Phys. Rev. A **33**, 2047 (1986). These authors explicitly assume frictionless contact between the polymer and the gel.
[19] M. O. de la Cruz, D. Gersappe, and E. O. Shaffer, Phys. Rev. Lett. **64**, 324 (1990).
[20] E. O. Shaffer and M. O. de la Cruz, Macromolecules **22**, 1351 (1989).
[21] T. A. J. Duke, Phys. Rev. Lett. **62**, 2877 (1989); J. Chem. Phys. **93**, 9055 (1990).
[22] T. L. Madden and J. M. Deutsch, J. Chem. Phys. **94**, 1584 (1991).
[23] J. M. Deutsch and J. D. Reger, J. Chem. Phys. **95**, 2065 (1991).
[24] T. A. J. Duke and J. L. Viovy, Phys. Rev. Lett. **68**, 542 (1992); J. Chem. Phys. **96**, 8552 (1992).
[25] G. W. Slater, J. Physique II (France) **2**, 1149 (1992).
[26] C. R. Calladin, C. M. Collis, H. R. Drew, and M. R. Mott, J. Mol. Biol. **221**, 981 (1991); see also E. Avranitdou and D. Hoagland, Phys. Rev. Lett.

67, 1461 (1991) and D. L. Smisek and D. A. Hoagland, Science **248**, 1221 (1990).
[27] D. C. Schwartz, W. Safran, J. Haas, R. M. Goldenberg, and C. R. Cantor, Cold Spring Harb. Symp. Quant. Biol. **47**, 189 (1983).
[28] D. C. Schwartz and C. R. Cantor, Cell **37**, 67 (1984).
[29] M. V. Olson, in *Genetic Engineering*, edited by J. K. Setlow (Plenum, New York, 1989), pp. 183, 227.
[30] D. Vollrath and R. W. Davies, Nucleic Acids Res. **15**, 7865 (1987).
[31] C. Turmel, E. Brassard, G. W. Slater, and J. Noolandi, Nucleic Acids Res. **18**, 569 (1990).
[32] C. L. Smith and C. L. Cantor, Methods Enzymol. **155**, 449 (1987).
[33] S. B. Smith and A. J. Bendich, Biopolymers **29**, 1167 (1990).
[34] S. F. Burlatsky and J. M. Deutch, Science **260**, 1782 (1993).
[35] P. G. de Gennes, C. R. Acad. Sci. B **228**, 212 (1979); J. N. Israelachvili, *Intermolecular and Surface Forces* (Academic, London, 1993).
[36] Harrison, C. A. White, R. J. Colto, and D. W. Brener, Phys. Rev. B **46**, 9700 (1992).
[37] R. M. Overney, H. Takano, M. Fujihira, W. Paulus, and H. Ringsdorf, Phys. Rev. Lett. **72**, 3546 (1994).
[38] W. D. Volkmuth, T. Duke, M. C. Wu, R. H. Austin, and A. Szabo, Phys. Rev. Lett. **72**, 2117 (1994).
[39] N. H. Frank, *Introduction to Mechanics and Heat* (McGraw-Hill, New York, 1939), p. 55.
[40] One can prove that if a segment size is higher than a fiber diameter successive segments which interact with the same fiber provide one effective interaction. Therefore results of this section are valid for any fiber diameter and segment size.
[41] The same result can be obtained for any $\delta r > a$. For example, let us consider the chain fragment with $\delta r = 2a$, which is depicted in Fig. 3. It contains 12 segments, only three of which interact with fibers. Since both segments with numbers 1 and 12 are at the boundary of the coarse graining interval, only one is included in the number of interactions for this interval, the other segment contributes to the neighboring interval with segment indexes smaller then 1 (or bigger then 12). Therefore the total number of interactions for this fragment is equal to 2. The length of a given fragment along the path is equal to $2a$, since a is equal to the length of the primitive path step and we have two path steps for this fragment. Coarse grained leaner density $\rho = 12/(2a) = 6/a$. The probability of interaction ϵ is equal to the number of the interactions divided by the total number of segments, i.e., to 1/6, which equals to $1/(\rho a)$.
[42] When the segment velocity approaches zero, it is necessary to take into account the influence of thermal fluctuation which are not included in our analysis. These thermal fluctuations will lead to polymer motion therefore modifying the results quoted here as $v = 0$. However, one can show that in this case the velocity does not depend on external force, and, therefore, the mobility equals to zero.
[43] Conclusions for both nonsymmetrical and symmetrical configuration are similar. However for the nonsymmetrical configuration the opportunity to ''unfreeze'' a trapped chain by a change of the field direction is more explicit [see Eqs. (31) and (69) and the discussion below them.]
[44] S. B. Smith, P. K. Aldridge, and J. B. Callis, Science **243**, 203 (1989).
[45] The coarse graining excludes end effects which lead to small corrections that do not depend on polymer length.
[46] S. D. Levene and B. H. Zimm, Proc. Nat. Acad. Sci. **84**, 4054 (1987).
[47] P. de Gennes, *Scaling Concepts in Polymer Physics* (Cornell University, Itaca and London, 1979), pp. 19–21.
[48] For $v = 0$ and typical values of $\cos\Theta$ [see Eq. (69)] we obtain that the limiting tension Eq. (65) is smaller then the tension in free dragging limit Eq. (66) if $n^2 > N_{BR} s a/b^2$ where $N_{BR} = (qEa/W)^{-2}$ is the borderline number of segments which determines the transition from inverse L to constant dependence of mobility in biased reptation theory in the absence of solid friction. The chain remains harmonic, i.e., nonstretched if $f < \gamma l$ which leads to $al^2 N_{BR} > sb^2$.
[49] Reduction of tension for long chains in gels with high concentration (and, therefore, with large solid friction) was observed experimentally. J. L. Viovy, private communication.
[50] R. I. Tanner, *Engineering Reology* (Oxford University, Oxford, 1985).
[51] If the length of the trailing arm becomes larger then the mobility threshold, the tension determined from the static equations presented below apparently becomes negative, since the tension changes sign i at the turning point.
[52] F. U. Gast and H. L. Sänger, Electrophoresis **15** 1493 (1994).
[53] In some off lattice simulation (Refs. 18–22), the rules for chain movement include rejection of the move (in contrast to elastic reflection) if the chain encounters a gel point. This implicitly corresponds to an inelastic collision which is required for solid friction.